

Accelerated Multiparameter Mapping Using Low-Rank Tensors

Anthony G. Christodoulou¹ and Zhi-Pei Liang¹

¹Beckman Institute and Department of Electrical and Computer Engineering, University of Illinois at Urbana-Champaign, Urbana, IL, United States

INTRODUCTION

Multiparameter mapping is a powerful tool for measuring multiple tissue properties (e.g., ρ , T_1 , T_2 , T_2^*) for quantitative tissue characterization [1]. However, multiparameter mapping suffers from the well-known curse of dimensionality (each new parameter being mapped adds another dimension to the image function, so the number of unknowns grows exponentially). As a result, practical applications of multiparameter mapping have been limited due to long data acquisition time. Low-rank matrix modeling and compressed sensing have proved useful for parametric mapping, but they have not explicitly and fully exploited the underlying low-rank tensor structure induced by the partial separability of the multivariate function to be imaged. This paper presents a novel tensor-based data acquisition and reconstruction method for highly accelerated multiparameter mapping. We will demonstrate the proposed method in FLASH-based ρ , T_1 , and T_2^* mapping of an *ex vivo* rat heart infiltrated by superparamagnetic iron oxide (SPIO)-labeled macrophages.

METHODS

We model the multivariate image function as partially separable in space, flip angle, and echo time [2]:

$$\rho(\mathbf{r}, \alpha, TE) = \sum_{\ell=1}^L \sum_{m=1}^M \sum_{n=1}^N c_{\ell m n} u_{\ell}(\mathbf{r}) v_m(\alpha) w_n(TE) \quad (1)$$

This decomposition can be viewed as representing ρ as a low-rank tensor, or more precisely, as a rank- (L, M, N) tensor [3]. This model motivates a data acquisition strategy wherein we collect navigator data by densely sampling (\mathbf{k}, α, TE) -space over very limited locations of (\mathbf{k}, α) -space and (\mathbf{k}, TE) -space, and imaging data by sparsely sampling the remainder of (\mathbf{k}, α, TE) -space.

For the basic PS model, it is common to determine the subspace structure from the singular value decomposition (SVD) of a Casorati matrix containing navigator data. For this higher-order PS model, the navigator data from the densely sampled (\mathbf{k}, α) -space and (\mathbf{k}, TE) -space locations enable the definition of two “Casorati tensors”. We collapse the Casorati tensors along different dimensions (either the α or TE dimensions), forming two Casorati matrices: \mathbf{C}_1 , the j th column of which contains the samples $d\left(\{\mathbf{k}_p\}_{p=1}^P, \alpha_j, \{TE_p\}_{p=1}^P\right)$, where $\left(\{\mathbf{k}_p, TE_p\}_{p=1}^P\right)$ is the set of (\mathbf{k}, TE) -space locations that contain data from all flip angles; and \mathbf{C}_2 , the j th column of which contains the samples $d\left(\{\mathbf{k}_q\}_{q=1}^Q, \{\alpha_q\}_{q=1}^Q, TE_j\right)$, where $\left(\{\mathbf{k}_q, \alpha_q\}_{q=1}^Q\right)$ is the set of (\mathbf{k}, α) -space locations that contain data from all echo times. The M most significant right singular vectors of \mathbf{C}_1 yield basis functions $\{v_m(\alpha)\}_{m=1}^M$; the N most significant right singular vectors of \mathbf{C}_2 yield basis functions $\{w_n(TE)\}_{n=1}^N$.

It is simple to show that the decomposition in Eq. 1 can be expressed as: $\rho(\mathbf{r}, \alpha, TE) = \sum_{\ell=1}^L u_{\ell}(\mathbf{r}) \psi_{\ell}(\alpha, TE)$, where $\psi_{\ell}(\alpha, TE) = \sum_{m=1}^M \sum_{n=1}^N c_{\ell m n} v_m(\alpha) w_n(TE)$. Without knowledge of the c , we can define $\hat{\mathbf{L}} = MN$ functions $\hat{\psi}_{\ell}(\alpha, TE) = \hat{\psi}_{m,n}(\alpha, TE) = v_m(\alpha) w_n(TE)$ (where ℓ indexes the Cartesian set of m, n pairings). Noting that $\{\hat{\psi}_{\ell}(\alpha, TE)\}_{\ell=1}^L$ defines a tensor-product subspace that contains the subspace spanned by $\{\psi_{\ell}(\alpha, TE)\}_{\ell=1}^L$, we can use $\rho(\mathbf{r}, \alpha, TE) = \sum_{\ell=1}^L u_{\ell}(\mathbf{r}) \hat{\psi}_{\ell}(\alpha, TE)$ for image reconstruction. More specifically, we solve the following optimization problem to recover $\{u_{\ell}(\mathbf{r})\}_{\ell=1}^L$ from the imaging data sparsely sampling (\mathbf{k}, α, TE) -space:

$$\arg \min_{\{u_{\ell}(\mathbf{r})\}_{\ell=1}^L} \left\| \mathbf{d} - \Omega \left\{ \sum_{\ell=1}^L \mathcal{F}_{\mathbf{r}}\{u_{\ell}(\mathbf{r})\} \hat{\psi}_{\ell}(\alpha, TE) \right\} \right\|_2^2 + R(\{u_{\ell}(\mathbf{r})\}_{\ell=1}^L),$$

where \mathbf{d} is the vector of measured data, Ω is the sparse sampling operator, and R is a regularization function, which can be chosen to be a weighted L2 penalty function or sparsity-promoting L1 penalty.

RESULTS AND DISCUSSION

We used 200×200 gold standard images defined for 10 flip angles ($2^\circ, 5^\circ, 10^\circ, 15^\circ, 20^\circ, 25^\circ, 30^\circ, 35^\circ, 40^\circ$, and 45°) and 11 echo times (0.025, 0.050, 0.075, 0.1, 0.25, 0.50, 0.75, 1, 2.5, 5, and 7.5 ms) using a FLASH sequence signal model. We compared two navigator sampling strategies: 1) dense sampling of (\mathbf{k}, α, TE) -space over an 8×200 \mathbf{k} -space region; and 2) dense sampling of (\mathbf{k}, α, TE) -space over a 23×200 \mathbf{k} -space region for two flip angles ($2^\circ, 45^\circ$) and two echo times (0.025 ms, 7.5 ms). The two strategies collect the same amount of navigator data. We randomly undersampled the remainder of (\mathbf{k}, α, TE) -space by a factor of 18.3 for a total undersampling factor of 10.8.

Figures 1 and 2 depict R_1 and R_2^* maps, respectively, from the gold standard and from the images accelerated using the proposed method. The regularization function R was chosen to impose anatomical edge constraints [4] generated from a composite image as in [5]. The T_1 - and T_2^* -shortening effect of the SPIO-labeled macrophages can clearly be seen in all cases. The proposed method accurately preserves the underlying T_1 and T_2^* tissue properties, with the exception of T_2^* values below 2 ms that are already challenging to accurately quantify. There were no significant differences in image quality between navigation strategies, demonstrating the flexible navigator sampling requirements of the proposed method.

CONCLUSION

This paper presents a novel tensor-based data acquisition and image reconstruction method for highly accelerated multiparameter mapping. The method will significantly enhance the practical utility of multiparameter mapping.

REFERENCES

[1] D. Ma, *et al.*, *Nature* 2013, pp. 187-92. [2] Z.-P. Liang, *IEEE-ISBI* 2007, pp. 988-91. [3] T. G. Kolda and B. W. Bader, *SIAM J Matrix Anal Appl* 2009, pp. 455-500. [4] J. P. Haldar, *et al.*, *MRM* 2008, pp. 810-8. [5] A. G. Christodoulou, *et al.*, *IEEE-EMBC* 2010, pp. 871-4.

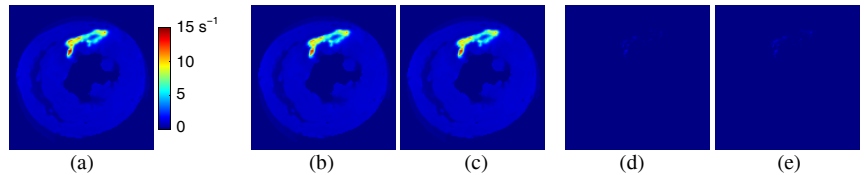


Fig. 1: R_1 maps from (a) the gold standard and 10.8x-accelerated images using (a) navigator strategy 1, and (b) navigator strategy 2. (d) and (e) are error maps for (b) and (c), respectively.

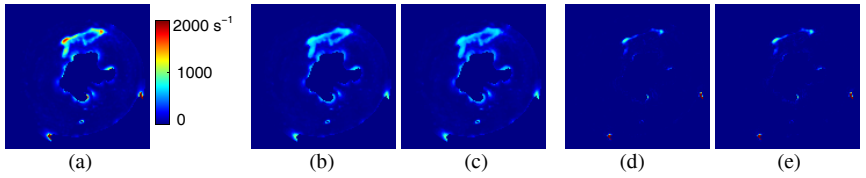


Fig. 2: R_2^* maps from (a) the gold standard and 10.8x-accelerated images using (a) navigator strategy 1, and (b) navigator strategy 2. (d) and (e) are error maps for (b) and (c), respectively.